Inorg. Chem. **2008**, *47*, 5978−5987

Halide Addition/Abstraction in Phosphido Derivatives: Isolation of the Thallium and Silver Intermediates[†,‡]

Juan Forniés,* Consuelo Fortuño, Susana Ibáñez, and Antonio Martín

Departamento de Química Inorgánica, Instituto de Ciencia de Materiales de Aragón, Universidad de Zaragoza-C.S.I.C., E-50009 Zaragoza, Spain

Received February 15, 2008

Reaction of unsaturated (44e$^-$ skeleton) $[PdPt_2(\mu\text{-}PPh_2)_2(\mu\text{-}P_2Ph_4)(R_F)_4]$ **4** with Br^- produces the saturated (48e$^-$ skeleton) complex $[NBu_4][(R_F)_2Pt(\mu\text{-}PPh_2)(\mu\text{-}Br)Pd(\mu\text{-}PPh_2)(\mu\text{-}P_2Ph_4)Pt(R_F)_2]$ **5** without any M−M′ bond. Attempts to eliminate Br^- of **5** with Ag^+ in CH_2Cl_2 as a solvent gives a mixture of $[(R_F)_2Pt^{III}(\mu\text{-}PPh_2)_2Pt^{III}(R_F)_2]$ and some other unidentified products as a consequence of oxidation and partial fragmentation. However, when the reaction of **5** with Ag^+ is carried out in CH_3CN, no oxidation is observed but the elimination of Br^- and the formation of $[(R_F)_2(CH_3CN)Pt(\mu\text{-}PPh_2)Pd(\mu\text{-}PPh_2)(\mu\text{-}P_2Ph_4)Pt(R_F)_2]$ **6** (46e$^-$ skeleton), a complex with a Pt−Pd bond, takes place. It is noteworthy that the reaction of **5** with $TlPF_6$ in CH_2Cl_2 does not precipitate TlBr but forms the adduct $[(R_F)_2PtTl(\mu\text{-}PPh_2)(\mu\text{-}Br)Pd(\mu\text{-}PPh_2)(\mu\text{-}P_2Ph_4)Pt(R_F)_2]$ **7** with a Pt−Tl bond. Likewise, **5** reacts with $[AgOClO_3(PPh_3)]$ in CH_2Cl_2 forming the adduct $[AgPdPt_2(\mu\text{-}Br)(\mu\text{-}PPh_2)_2(\mu\text{-}Ph_2P\text{-}PPh_2)(R_F)_4(PPh_3)]$ **8**, which contains a Pt−Ag bond. Both adducts are unstable in a CH_3CN solution, precipitating TlBr or AgBr and yielding the unsaturated **6**. The treatment of $[NBu_4]_2[(R_F)_2Pt(\mu\text{-}PPh_2)_2Pd(\mu\text{-}PPh_2)_2Pt(R_F)_2]$ in CH_3CN with I_2 (1:1 molar ratio) at 233 K yields a mixture of **4** and **6**, which after recrystallization from CH_2Cl_2 is totally converted in **4**. If the reaction with I_2 is carried out at room temperature, a mixture of the isomers $[NBu_4][(R_F)_2Pt(\mu\text{-}PPh_2)(\mu\text{-}I)Pd(\mu\text{-}PPh_2)(\mu\text{-}P_2Ph_4)Pt(R_F)_2]$ **9** and $[NBu_4][(R_F)(PPh_2R_F)Pt(\mu\text{-}PPh_2)(\mu\text{-}I)Pd(\mu\text{-}PPh_2)_2Pt(R_F)_2]$ **10** are obtained. The structures of the complexes have been established on the bases of NMR data, and the X-ray structures of **5**-**8** have been studied. The relationship between the different complexes has been studied.

Introduction

Halide abstraction from a late transition metal center in the presence of a weakly coordinating anion is an activation procedure that is frequently used in chemistry. Recently, it has been suggested that the role of the silver salts toward some chloro derivatives of platinum as catalysts may extend beyond chloride abstraction,[1] and two complexes containing the Pd−Ag−Cl moiety have been proposed as intermediates in the precatalyst activation by chloride abstraction.[2]

In the course of our current research, we are focused on polynuclear phosphido derivatives of platinum and palladium(III) in which the metal centers surprisingly do not display octahedral environments.[3−5] This type of complex evolves easily toward the formation of platinum and palladium(II) derivatives through reductive coupling processes.[5,6] In some cases, halide addition to the platinum and palladium(III) derivatives is a way of inducing the coupling process to form platinum and palladium(II) complexes, which, in some cases, is a fully reversible process, that is, the abstraction of halide regenerates the platinum(III) complex.[6] In the same context, it is noteworthy that examples in

* To whom correspondence should be addressed. Fax: +34976761187. E-mail: juan.fornies@unizar.es.

† Polynuclear Homo- or Heterometallic Palladium(II)−Platinum(II) Pentafluorophenyl Complexes Containing Bridging Diphenylphosphido Ligands 24. For part 23 see ref 70.

‡ Dedicated to Professor Pascual Royo, Universidad de Alcalá, on the occasion of his 70th anniversary.

(1) Karshtedt, D.; Bell, A. T.; Tilley, T. D. *Organometallics* **2004**, *23*, 4169–4171.

(2) van Leeuven, P. W. N. M.; Zuideveld, M. A.; Swennenhuis, B. H. G.; Freixa, Z.; Kamer, P. C. J.; Goubitz, K.; Fraanje, J.; Lutz, M.; Spek, A. L. *J. Am. Chem. Soc.* **2003**, *125*, 5523–5539.

(3) Alonso, E.; Casas, J. M.; Cotton, F. A.; Feng, X. J.; Forniés, J.; Fortuño, C.; Tomás, M. *Inorg. Chem.* **1999**, *38*, 5034–5040.

(4) Alonso, E.; Casas, J. M.; Forniés, J.; Fortuño, C.; Martín, A.; Orpen, A. G.; Tsipis, C. A.; Tsipis, A. C. *Organometallics* **2001**, *20*, 5571–5582.

(5) Ara, I.; Chaouche, N.; Forniés, J.; Fortuño, C.; Kribii, A.; Tsipis, A. C. *Organometallics* **2006**, *25*, 1084–1091.

(6) Chaouche, N.; Forniés, J.; Fortuño, C.; Kribii, A.; Martín, A.; Karipidis, P.; Tsipis, A. C.; Tsipis, C. A. *Organometallics* **2004**, *23*, 1797–1810.

10.1021/ic800294c CCC: $40.75
Published on Web 05/23/2008

Scheme 1

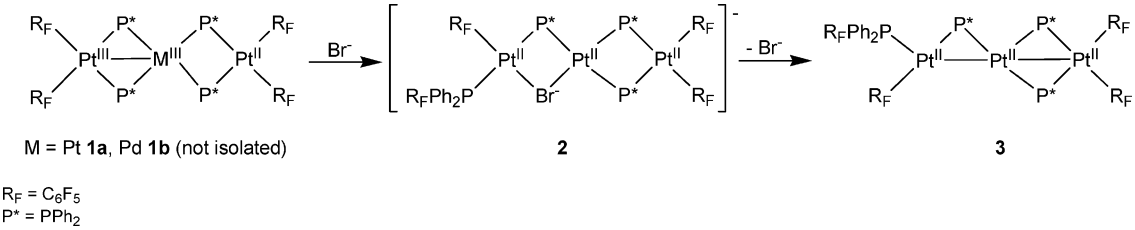

Scheme 2

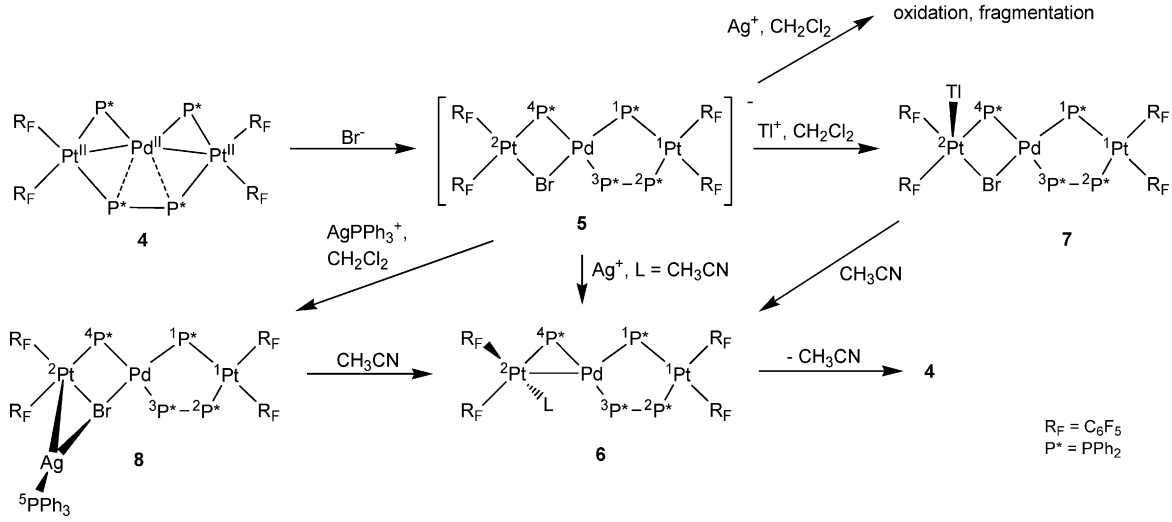

which the abstraction of halide from phosphido platinum or palladium(II) derivatives imply reductive coupling with P−C bond formation to form platinum or palladium(I) complexes are known.[7–9]

As far as the trinuclear complexes are concerned, the solid-state structure and its behavior toward Br^- of the platinum complex $[(R_F)_2Pt^{III}(\mu\text{-}PPh_2)_2Pt^{III}(\mu\text{-}PPh_2)_2Pt^{II}(R_F)_2]$ (R_F = C_6F_5, **1a**) were shown in Scheme 1.[10] This behavior in the addition/elimination of halide has been also observed in some tetranuclear platinum(II) derivatives.[11] Nevertheless, when we tried to synthesize the analogous heterotrinuclear palladium/platinum(III) $[(R_F)_2Pt^{III}(\mu\text{-}PPh_2)_2Pd^{III}(\mu\text{-}PPh_2)_2\text{-}Pt^{II}(R_F)_2]$ **1b** the isolated solid was in fact the palladium/platinum(II) $[PdPt_2(\mu\text{-}PPh_2)_2(\mu\text{-}Ph_2P\text{-}PPh_2)(R_F)_4]$ (**4**), an isomer of **1b**, and its solid-state structure (X-ray) is depicted in Scheme 2.[12] As can be seen, the coupling of two bridging phosphido ligands forms tetraphenyldiphosphine in a very unusual process. We established, from NMR studies in solution, and in line with the theoretical calculations, that at room temperature the Pd−P and P−P bonds in **4** are highly delocalized.[12] These results indicate that the structure of **4** in solution at room temperature could be considered as a combination of that shown in Scheme 1 for **1b** (not isolable in the solid state) and the one found in the crystal structure **4**. To explore the conditions that favor a PPh_2/R_F coupling (formation of PPh_2R_F) versus the PPh_2/PPh_2 one (formation of P_2Ph_4), we have carried out the addition of bromide to **4** and its subsequent abstraction with thallium(I) and silver(I) salts as well as performing the oxidation of the heterotrinuclear palladium and platinum(II) $[NBu_4]_2[(R_F)_2Pt(\mu\text{-}PPh_2)_2Pd(\mu\text{-}PPh_2)_2Pt(R_F)_2]$ complex with I_2.

Results and Discussion

Synthesis. The reaction of a red suspension of $[PdPt_2(\mu\text{-}PPh_2)_2(\mu\text{-}Ph_2P\text{-}PPh_2)(R_F)_4]$ (**4**) in acetone with NBu_4Br (1:1 molar ratio) at room temperature produces a solution from which the anionic bromo derivative $[NBu_4][(R_F)_2Pt(\mu\text{-}PPh_2)(\mu\text{-}Br)Pd(\mu\text{-}PPh_2)(\mu\text{-}P_2Ph_4)Pt(R_F)_2]$ (**5**) is isolated (Scheme 2). The starting material **4** is an unsaturated trinuclear complex with a 44 valence electron count and, hence, with two platinum−palladium bonds. The coordination of the Br^- group as a bridging ligand (four electron donor) in **5** raises up the valence electron count to 48, and **5** is a saturated derivative, which does not require any Pt−Pd bonds. The addition of bromide to **4** rearranges the Pt−P and P−P bonding system, but the P−P bond of the diphosphine is maintained and the formation of a complex analogous to **2**, which would result from the breaking of the P−P bond and formation of a P−C bond (formation of PPh_2R_F), is not observed.

The addition of $AgClO_4$ to the bromo derivative **5** gives different results if dichloromethane or acetonitrile is used

(7) Falvello, L. R.; Forniés, J.; Fortuño, C.; Martín, A.; Martínez-Sariñena, A. P. *Organometallics* **1997**, *16*, 5849–5856.
(8) Albinati, A.; Filippi, V.; Leoni, P.; Marchetti, L.; Pasquali, M.; Passarelli, V. *Chem. Commun.* **2005**, 2155–2157.
(9) Archambault, C.; Bender, R.; Braunstein, P.; Decian, A.; Fischer, J. *Chem. Commun.* **1996**, 2729–2730.
(10) Forniés, J.; Fortuño, C.; Ibáñez, S.; Martín, A. *Inorg. Chem.* **2006**, *45*, 4850–4858.
(11) Forniés, J.; Fortuño, C.; Gil, R.; Martín, A. *Inorg. Chem.* **2005**, *44*, 9534–9541.
(12) Forniés, J.; Fortuño, C.; Ibáñez, S.; Martín, A.; Tsipis, A. C.; Tsipis, C. A. *Angew. Chem., Int. Ed.* **2005**, *44*, 2407–2410.

as a solvent. The yellow solid obtained from dichloromethane is a mixture of products that we have not been able to separate but the $^{31}P\{^1H\}$ NMR spectrum of the mixture indicates the presence of the well-known dinuclear platinum(III) derivative $[(R_F)_2Pt^{III}(\mu\text{-}PPh_2)_2Pt^{III}(R_F)_2]$[3] as well as some unidentified species, which seem to contain the $Pd(\mu\text{-}PPh_2)(\mu\text{-}Ph_2P\text{-}PPh_2)Pt$ fragment. This indicates that the reaction progresses with oxidation of the platinum(II) center along with fragmentation of the trinuclear complex (Scheme 2). It is well-known that the strength of the silver(I) ion as a one-electron oxidant is solvent dependent. It is a strong oxidant in CH_2Cl_2, whereas its formal potential is considerably decreased in NCMe.[13–15] Addition of $AgClO_4$ to the bromoderivative **5** in acetonitrile produces a different result because the silver acts as a bromide scavenger, and the acetonitrile, a donor solvent, coordinates to the metal centers and an insoluble crude yellow solid, which turns orange-pink when dried, crystallizes. Recrystallization from CH_2Cl_2 to separate the AgBr affords an orange-pink solid $[(R_F)_2(CH_3CN)Pt(\mu\text{-}PPh_2)Pd(\mu\text{-}PPh_2)(\mu\text{-}P_2Ph_4)Pt(R_F)_2]$ (**6**), which, with a coordinated CH_3CN ligand, shows a 46 valence electron count and hence a Pt−Pd bond (Scheme 2). The process reveals that the yellow solid could be an acetonitrile adduct of **6**, which easily eliminates the ligand. In addition, cluster **4** slowly crystallizes from solutions of **6** in CH_2Cl_2 (Scheme 2). The easy elimination of the acetonitrile ligand in transition-metal complexes is a process that is commonly observed.[16] Although **4** is insoluble in acetonitrile, addition of a few drops of $CHCl_3$ to an orange suspension of **4** in CH_3CN allows isolation of **6**. From these reactions, it can be concluded that the addition/abstraction of bromide and acetonitrile are fully reversible processes, and the cleavage of the P−P bond is not observed.

Although silver and thallium salts are often used interchangeably as halide abstractors, the oxidation sensitive nature of **5** suggests the use of a thallium(I) salt to study a possible activation procedure from **5** in CH_2Cl_2. The addition of $TlPF_6$ to dichloromethane solutions of **5** does not cause the elimination of TlBr, but the complex $[PdPt_2Tl(\mu\text{-}Br)(\mu\text{-}PPh_2)_2(\mu\text{-}Ph_2P\text{-}PPh_2)(R_F)_4]$ (**7**), an unexpected adduct of Tl^+ and **5** (Scheme 2), is isolated. **7** is not stable in acetonitrile and evolves to **6** (Scheme 2). Considering the proven efficiency of thallium(I) salts for bromide abstraction, the formation of **5** is rather surprising. Structurally characterized complexes displaying Pt−Tl bonds are known[17–34] but metal-halo complexes that also contain thallium centers are very scarce. Tetrametallic M_2Tl_2 (M = Pd, Pt) complexes with M−Cl−Tl bonds and without M···Tl interactions have been recently proposed as possible intermediates in the general chloride abstraction process.[28] A Ni_3Tl cluster in which a Tl−I moiety is μ_3-capping three nickel centers through Ni−Tl bonds has been characterized.[35] **7**, showing a Br−Pt−Tl system, is well related to the unprecedented Cl−Pt−Tl adduct from $[Pt(CH_2Ph)Cl(PCH_2\text{-}ox)]$ and Tl^+, reported by Braunstein.[29] It is to be noted that in this case the analogous Cl−Pt−Ag is not obtained but elimination of AgCl is observed.[29] As previously stated, we have been able to isolate the adduct of **4** with thallium(I), **7**, but not an analogous adduct with silver(I) due probably to the oxidation process in CH_2Cl_2. Taking into account that different silver fragments show different oxidation potentials and aiming to achieve the coordination of silver(I) rather than the oxidation of platinum(II), we have carried out the reaction of **5** with $[AgOClO_3(PPh_3)]$ in CH_2Cl_2 (1:1 molar ratio) to synthesize the adduct **5**·$Ag(PPh_3)^+$ and the complex $[AgPd_2Pt_2(\mu\text{-}Br)(\mu\text{-}PPh_2)_2(\mu\text{-}Ph_2P\text{-}PPh_2)(R_F)_4(PPh_3)]$ (**8**) with a Pt(II)−Ag(I) bond is obtained (Scheme 1). **8** eliminates AgBr in acetonitrile, giving **6**. The reactions of **5** with M(I) (M = Ag, Tl) indicate that both the halide abstraction and the oxidation could start with a coordination process, giving rise to intermediates with Pt−M bond.[12]

All of these results indicate that once the tetraphenyldiphosphine is formed in **4** (from the complex $[(R_F)_2Pt^{II}(\mu\text{-}PPh_2)_2Pd^{II}(\mu\text{-}PPh_2)_2Pt^{II}(R_F)_2]^{2-}$ with Ag^+ as oxidizing agent),[12] the P−P bond is maintained, and formation of P−C bond does not take place in either of the cases.

To broaden the scope of this study, we have also carried out the reaction of $[NBu_4]_2[(R_F)_2Pt^{II}(\mu\text{-}PPh_2)_2Pd^{II}(\mu\text{-}PPh_2)_2Pt^{II}(R_F)_2]$ with I_2 (1:1 molar ratio) as an oxidizing agent, in acetonitrile. When the reaction is carried out at 233 K, a solid, which was identified as a mixture of **4** and **6**, was obtained. After recrystallization from CH_2Cl_2 at room temperature, the mixture was completely reverted to the neutral, acetonitrile free cluster **4**. From the mother liquors of the reaction at 233 K, a solid was recovered, and the

(13) Connelly, N. G.; Geiger, W. E. *Chem. Rev.* **1996**, *96*, 877–910.
(14) Ebihara, M.; Iiba, M.; Matsuoka, H.; Okuda, C.; Kawamura, T. *J. Organomet. Chem.* **2004**, *689*, 146–153.
(15) Song, L.; Trogler, W. *Angew. Chem., Int. Ed.* **1992**, *31*, 770–772.
(16) Murahashi, T.; Nagai, T.; Okuno, T.; Matsutani, T.; Kurosawa, H. *Chem. Commun.* **2000**, 1689–1690.
(17) Berenguer, J. R.; Forniés, J.; Gil, B.; Lalinde, E. *Chem.—Eur. J.* **2006**, *12*, 785–795.
(18) Catalano, V. C.; Malwitz, M. A. *J. Am. Chem. Soc.* **2004**, *126*, 6560–6561.
(19) Charmant, J. P. H.; Forniés, J.; Gómez, J.; Lalinde, E.; Merino, R. I.; Orpen, A. G. *Organometallics* **2003**, *22*, 652–656.
(20) Mednikov, E. G.; Dahl, L. F. *Dalton Trans.* **2003**, 3117–3125.
(21) Stadnichenko, R.; Sterenberg, B. T.; Bradford, A. M.; Jennings, M. C.; Puddephatt, R. J. *Dalton Trans.* **2002**, 1212–1216.
(22) Ara, I.; Berenguer, J. R.; Forniés, J.; Gómez, J.; Lalinde, E.; Merino, R. I. *Inorg. Chem.* **1997**, *36*, 6461–6464.
(23) Usón, R.; Forniés, J.; Tomás, M.; Garde, R.; Merino, R. I. *Inorg. Chem.* **1997**, *36*, 1383–1387.
(24) Hao, L.; Vittal, J. J.; Puddephatt, R. J. *Organometallics* **1996**, *15*, 3115–3123.
(25) Usón, R.; Forniés, J.; Tomás, M.; Garde, R. *J. Am. Chem. Soc.* **1995**, *117*, 1837–1837.
(26) Silva, N. d.; FryC. G.; Dahl, L. F. *Dalton Trans.* **2006**, 1051–1059.
(27) Falvello, L. R.; Forniés, J.; Garde, R.; García, A.; Lalinde, E.; Moreno, M. T.; Steiner, A.; Tomás, M.; Usón, I. *Inorg. Chem.* **2006**, *45*, 2543–2552.
(28) Devic, T.; Batail, P.; Fourmigué, M.; Avarvari, N. *Inorg. Chem.* **2004**, *43*, 3136–3141.
(29) Oberbeckmann-Winter, N.; Braunstein, P.; Welter, R. *Organometallics* **2004**, *23*, 6311–6318.
(30) Chen, W.; Liu, F.; Xu, D.; Matsumoto, K.; Kishi, S.; Kato, M. *Inorg. Chem.* **2006**, *45*, 4552–5560.
(31) Stork, J. R.; Olmsread, M. M.; Fettinger, J. C.; Balch, A. L. *Inorg. Chem.* **2006**, *45*, 849–857.
(32) Ma, G.; Kritikos, M.; Maliarik, M.; Glaser, J. *Inorg. Chem.* **2004**, *43*, 4328–4340.
(33) Catalano, V. C.; Bennett, B. L.; Yson, R. L.; Noll, B. C. *J. Am. Chem. Soc.* **2000**, *122*, 10056–10062.
(34) Song, H.-B.; Zhang, Z.-Z.; Hui, Z.; Che, C.-M.; Mak, T. C. W. *Inorg. Chem.* **2002**, *41*, 3146–3154.
(35) Johnson, M. J. A.; Gantzel, P. K.; Kubiak, C. P. *Organometallics* **2002**, *21*, 3831–3832.

Scheme 3

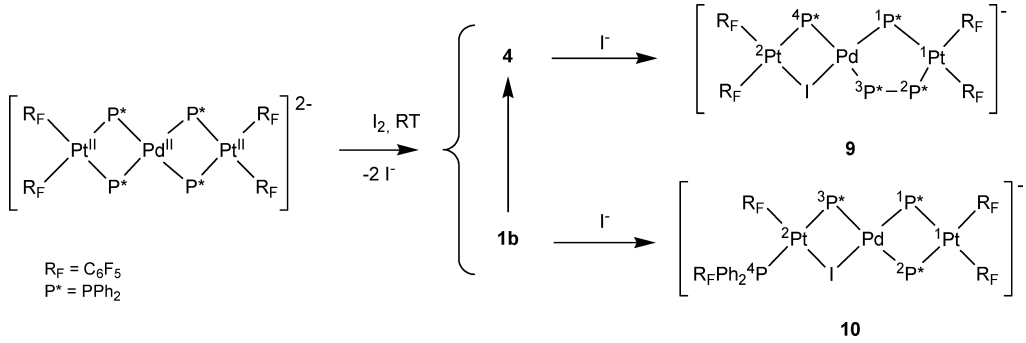

spectroscopic study shows it to be mainly the starting material along with a small amount of unidentified products. Their ^{19}F NMR spectrum unambiguously rules out the presence of PPh_2R_F, that is, the formation of the P−C bond does not take place. Nevertheless, when the reaction is carried out at room temperature for 7 h, the resulting solid, after work up, is identified as a mixture of two anionic isomers $[NBu_4][(R_F)_2Pt(\mu\text{-}PPh_2)(\mu\text{-}I)Pd(\mu\text{-}PPh_2)(\mu\text{-}P_2Ph_4)Pt(R_F)_2]$ (**9**) and $[NBu_4][(R_F)_2Pt(\mu\text{-}PPh_2)_2Pd(\mu\text{-}PPh_2)(\mu\text{-}I)PtR_F(PPh_2R_F)]$ (**10**) (Scheme 3). This indicates that, at room temperature, reductive coupling with P−P or P−C bond formation takes place. Although we have been not able to separate them, their characterization can be unambiguously carried out from their $^{31}P\{^1H\}$ NMR spectrum in solution. The data assigned to **9** compare well with those of **5**, and those due to **10** compare well with the values of the analogous homotrinuclear $[NBu_4][(R_F)_2Pt(\mu\text{-}PPh_2)_2Pt(\mu\text{-}PPh_2)(\mu\text{-}I)PtR_F(PPh_2R_F)]$ previously reported.[10] **9** is analogous to **5**, and its formation can be easily understood as the result of adding I^- to **4**, as in the synthesis of **5**. Furthermore, **10** contains a PPh_2R_F ligand but not a P_2Ph_4 one. We have already observed that the reductive coupling between PPh_2 and C_6F_5 fragments does not take place from **4**, but rather from the oxidation of the platinum/palladium(II) complex $[(R_F)_2Pt^{II}(\mu\text{-}PPh_2)_2Pd^{II}(\mu\text{-}PPh_2)_2Pt^{II}(R_F)_2]^{2-}$ with I_2, that is, in this process, the probable intermediate oxidized **1b** (Scheme 1) displays two possible paths of reactions involving two reductive couplings: PPh_2/C_6F_5 or PPh_2/PPh_2, with formation of P−C or P−P bonds respectively. When the reaction is carried out at 233 K, the I^- group does not coordinate and **1b** evolves via the formation of a P−P bond and the weakening of two Pd−P bonds, giving **4**. At higher temperature, the I^- group coordinates to the M(II) of **4**, giving **9** as expected. More interestingly, the I^- group also coordinates to the M(III) of **1b**, giving **10** through a PPh_2/C_6F_5 reductive coupling process,[10] and the formation of two additional M−I (M = Pt, Pd) bonds.[36]

X-ray Diffraction Studies. The crystal structures of **5**−**8** have been determined by X-ray diffraction methods. Crystal data and other details of the structure analyses are presented in Table 1. Selected bond distances and angles for these structures are listed in Tables 2–5. In the case of $[NBu_4][(R_F)_2Pt(\mu\text{-}PPh_2)(\mu\text{-}Br)Pd(\mu\text{-}PPh_2)(\mu\text{-}P_2Ph_4)Pt(R_F)_2]$ (**5**), the structural determination (Figure 1) confirms the trinuclear nature of the anion of **5**, with the three metal atoms disposed in an almost linear array [Pt(1)−Pd−Pt(2) = 158.2(1)°]. The metal centers lie in the center of square planar environments in such a way that the core of the anion is not planar. The dihedral angles are 25.5(1)° for the best platinum(1) and palladium planes and 49.5(1)° for the platinum(2) and palladium ones. The intermetallic separations [Pt(1)···Pd = 4.037(1) Å, Pt(2)···Pd = 3.302(1) Å] discard any kind of bonding interaction among the metal centers. Platinum(1) and palladium are bridged by a diphenylphosphido [P(1)] and a tetraphenyldiphosphane [P(2), P(3)] ligand. The presence of the bridging diphosphane ligand causes a long separation between platinum(1) and palladium and a considerable broadening of the Pt(1)−P(1)−Pd angle, which takes a value of 119.4(1)°. Furthermore, as expected, the two phosphorus atoms of the P_2Ph_4 group and the metals bridged by them do not lie in the same plane, the torsion angle being Pt(1)−P(2)−P(3)−Pd = 36.0(2)°. Palladium and platinum(2) are bridged by a diphenylphosphido and a bromo ligands. It is noteworthy that, in this case, the Pt(2)−P(4)−Pd angle is much narrower [91.1(1)°] than the analogous Pt(1)−P(1)−Pd mentioned above.

The crystal structure of $[(R_F)_2(CH_3CN)Pt(\mu\text{-}PPh_2)Pd(\mu\text{-}PPh_2)(\mu\text{-}P_2Ph_4)Pt(R_F)_2]$ (**6**) (Figure 2) again confirms its trinuclear nature and maintains the almost linear arrangement of the metal atoms [Pt(1)−Pd−Pt(2) = 162.8(1)°]. The $Pd(\mu\text{-}PPh_2)(\mu\text{-}P_2Ph_4)Pt(R_F)_2$ fragment is quite similar to the analogous one described above for **5**, with a Pt(2)−Pd distance of 3.988(1) Å (no metal−metal bond), a dihedral angle between the platinum(2) and palladium best environment planes of 26.5(1)°, quite a wide Pt(2)−P(2)−Pd angle [117.4(1)°], and a Pt(2)−P(4)−P(3)−Pd torsion angle of 55.9(1)°. Nevertheless, the environment of the palladium atoms and the geometry of the $(NCMe)(R_F)_2Pt(\mu\text{-}PPh_2)Pd$ fragment is noteworthy. The palladium atom only has three ligands coordinated with some P−Pd−P angles, somewhat

(36) According to a referee's suggestion, we have studied the room temperature reaction of I^- with **4** in acetonitrile to exclude the formation of $PPh_2C_6F_5$. To a suspension of 64 mg of **4** in 10 mL of acetonitrile, NBu_4I (16 mg) was added. The solution was stirred for 16 h at room temperature, evaporated almost to dryness, and ^{i}PrOH was added. An orange solid crystallized, which was identified (IR and ^{19}F NMR) as **9**.

Table 1. Crystal Data and Structure Refinement for Complexes $[NBu_4][(R_F)_2Pt(\mu\text{-}PPh_2)(\mu\text{-}Br)Pd(\mu\text{-}PPh_2)(\mu\text{-}P_2Ph_4)Pt(R_F)_2]\cdot CH_2Cl_2\cdot 0.5n\text{-}C_6H_{14}$ (**5**·CH_2Cl_2·$0.5n$-C_6H_{14}), $[(R_F)_2(CH_3CN)Pt(\mu\text{-}PPh_2)Pd(\mu\text{-}PPh_2)(\mu\text{-}P_2Ph_4)Pt(R_F)_2]\cdot 1.5CH_2Cl_2$ (**6**·$1.5CH_2Cl_2$), $[PdPt_2Tl(\mu\text{-}Br)(\mu\text{-}PPh_2)_2(\mu\text{-}Ph_2P\text{-}PPh_2)(R_F)_4]\cdot 2.25CH_2Cl_2$ (**7**·$2.25CH_2Cl_2$), and $[AgPdPt_2(\mu\text{-}Br)(\mu\text{-}PPh_2)_2(\mu\text{-}Ph_2P\text{-}PPh_2)(R_F)_4(PPh_3)]\cdot 1.5n\text{-}C_6H_{14}$ (**8**·$1.5n$-C_6H_{14})

	5·CH_2Cl_2·$0.5n$-C_6H_{14}	**6**·$1.5CH_2Cl_2$	**7**·$2.25CH_2Cl_2$	**8**·$1.5n$-C_6H_{14}
formula	$C_{88}H_{76}BrF_{20}NP_4PdPt_2$ ·CH_2Cl_2·$0.5n$-C_6H_{14}	$C_{74}H_{43}F_{20}NP_4PdPt_2$ ·$1.5CH_2Cl_2$	$C_{72}H_{40}BrF_{20}P_4PdPt_2Tl$ ·$2.25CH_2Cl_2$	$C_{90}H_{55}AgBrF_{20}P_5PdPt_2$ ·$1.5n$-C_6H_{14}
M_t [g mol^{-1}]	2355.88	2073.94	2380.86	2484.81
T [K]	100(1)	293(1)	100(1)	100(1)
λ [Å]	0.71073	0.71073	0.71073	0.71073
cryst syst	triclinic	triclinic	monoclinic	triclinic
space group	$P\bar{1}$	$P\bar{1}$	$P2_1/n$	$P\bar{1}$
a [Å]	10.9946(12)	12.4958(12)	15.293(2)	15.091(2)
b [Å]	18.396(2)	13.9499(15)	24.708(4)	18.759(3)
c [Å]	24.622(3)	21.957(3)	20.794(3)	19.315(3)
α [°]	110.168(2)	79.063(2)	90	102.123(3)
β [°]	97.111(2)	79.948(2)	90.277(3)	107.068(2)
μ [°]	100.760	87.795(4)	90	91.923(2)
V [Å^3]	4495.9(9)	3700.2(7)	7857(2)	5083.9(12)
Z	2	2	4	2
ρ [g cm^{-3}]	1.740	1.861	2.013	1.623
μ [mm^{-1}]	3.964	4.301	6.652	3.658
F(000)	2310	1998	4498	2418
2θ range [°]	3.5−50.1	3.0−50.1	2.6−50.0	3.4−50.0
no. of reflns collected	20 849	20 431	42 682	27 931
no. of unique reflns	15 112	12 881	13 864	17 656
R(int)	0. 0550	0.0238	0.0435	0.0247
final R indices [$I > 2\sigma(I)$][a]				
R_1	0.0668	0.0373	0.0373	0.0437
wR2	0.1182	0.0934	0.0898	0.1165
R indices (all data)				
R_1	0.1107	0.0476	0.0521	0.0621
wR2	0.1289	0.0958	0.0958	0.1268
GOF on F^2[b]	1.008	1.089	1.027	1.070

[a] $R_1 = \sum(|F_o| - |F_c|)/\sum |F_o|$. wR2 $= [\sum w(F_o^2 - F_c^2)^2 / \sum w(F_o^2)^2]^{1/2}$. [b] GOF $= [\sum w(F_o^2 - F_c^2)^2/(n_{obs} - n_{param})]^{1/2}$.

Table 2. Selected Bond Distances (Angstroms) and Angles (Degrees) for $[NBu_4][(R_F)_2Pt(\mu\text{-}PPh_2)(\mu\text{-}Br)Pd(\mu\text{-}PPh_2)(\mu\text{-}P_2Ph_4)Pt(R_F)_2]\cdot CH_2Cl_2\cdot 0.5n\text{-}C_6H_{14}$ (**5**·CH_2Cl_2·$0.5n$-C_6H_{14})

Pt(1)−C(1)	2.023(12)	Pt(1)−C(7)	2.042(12)	Pt(1)−P(2)	2.262(3)
Pt(1)−P(1)	2.369(3)	Pt(2)−C(19)	1.960(10)	Pt(2)−C(13)	2.061(11)
Pt(2)−P(4)	2.294(3)	Pt(2)−Br	2.531(1)	Pd−P(3)	2.307(3)
Pd−P(1)	2.307(3)	Pd−P(4)	2.334(4)	Pd−Br	2.563(2)
P(2)−P(3)	2.216(5)				
C(1)−Pt(1)−C(7)	83.9(5)			C(1)−Pt(1)−P(2)	88.8(4)
C(7)−Pt(1)−P(2)	172.5(3)			C(1)−Pt(1)−P(1)	178.0(3)
C(7)−Pt(1)−P(1)	94.6(4)			P(2)−Pt(1)−P(1)	92.7(1)
C(19)−Pt(2)−C(13)	88.4(4)			C(19)−Pt(2)−P(4)	97.3(3)
C(13)−Pt(2)−P(4)	172.8(3)			C(19)−Pt(2)−Br	177.3(4)
C(13)−Pt(2)−Br	92.5(3)			P(4)−Pt(2)−Br	82.0(1)
P(3)−Pd−P(1)	91.8(1)			P(3)−Pd−P(4)	165.9(1)
P(1)−Pd−P(4)	99.8(1)			P(3)−Pd−Br	88.2(1)
P(1)−Pd−Br	177.4(1)			P(4)−Pd−Br	80.5(1)
Pd−P(1)−Pt(1)	119.4(1)			P(3)−P(2)−Pt(1)	106.4(1)
P(2)−P(3)−Pd	114.6(2)				

distorted with respect to a square planar disposition. The Pt(1)−Pd distance is 2.885(1) Å, in the usual range for a metal−metal bond in this kind of complexes. However, the square plane formed by platinum(1) and the atoms of the ligands bonded to it is almost perpendicular to the best environment palladium plane [84.9(1)°]. This is a striking situation because, in this kind of polynuclear complexes with phosphido bridges and a metal−metal bond, this bond is usually contained in the same plane of the environments of the bonded metal atoms, which in turn, most frequently, are mutually coplanar. The acidic properties in palladium seem to be clear, in view of the lack of a ligand in the fourth coordination position. In fact, the platinum(1) atom can be regarded as the fourth ligand [platinum(1) is coplanar with palladium and the atoms bonded to it], thus completing the coordination sphere of palladium. The Pt(1)−P(1)−Pd angle has a value of 78.2(1)°, which is small, as is to be expected for a diphosphide group bridging two atoms joined by a metal−metal bond. The coordination sphere of platinum(1) is fairly typical and is completed by two terminal pentafluorophenyl groups and an acetonitrile ligand.

The crystal structure of $[PdPt_2Tl(\mu\text{-}Br)(\mu\text{-}PPh_2)_2(\mu\text{-}Ph_2P\text{-}PPh_2)(R_F)_4]$ (**7**) (Figure 3) shows that the $Pd(\mu\text{-}PPh_2)(\mu\text{-}P_2Ph_4)Pt(R_F)_2$ fragment is also similar to the analogous one described above for **5** and **6**. The Pt(1)−Pd−Pt(2) array is again almost linear [159.9(1)°], with a large Pt(1)−Pd distance [4.026(1) Å], wide Pt(1)−P(1)−Pd angle [119.5(1)°], and a Pt(1)−P(2)−P(3)−Pd torsion angle of 34.8(1)°. The other part of the complex, $(R_F)_2Pt(\mu\text{-}PPh_2)(\mu\text{-}Br)Pd$, is similar to the one described above for **5**, with a nonbonding

Table 3. Selected Bond Distances (Angstroms) and Angles (Degrees) for $[(R_F)_2(CH_3CN)Pt(\mu\text{-}PPh_2)Pd(\mu\text{-}PPh_2)(\mu\text{-}P_2Ph_4)Pt(R_F)_2]\cdot 1.5CH_2Cl_2$ (**6**·$1.5CH_2Cl_2$)

Pt(1)−C(1)	1.998(6)	Pt(1)−N	2.044(6)	Pt(1)−C(7)	2.080(6)
Pt(1)−P(1)	2.3299(18)	Pt(1)−Pd	2.8852(6)	Pt(2)−C(19)	2.069(6)
Pt(2)−C(13)	2.070(6)	Pt(2)−P(4)	2.2670(18)	Pt(2)−P(2)	2.3556(17)
Pd−P(1)	2.2458(18)	Pd−P(2)	2.3126(17)	Pd−P(3)	2.3523(18)
P(3)−P(4)	2.216(2)				
C(1)−Pt(1)−N	171.4(3)			C(1)−Pt(1)−C(7)	85.9(3)
N−Pt(1)-C(7)	91.2(2)			C(1)−Pt(1)−P(1)	90.77(19)
N−Pt(1)-P(1)	92.09(17)			C(7)−Pt(1)−P(1)	176.68(18)
C(1)−Pt(1)−Pd	96.68(19)			N−Pt(1)-Pd	91.37(17)
C(7)−Pt(1)−Pd	130.72(18)			P(1)−Pt(1)−Pd	49.62(4)
C(19)−Pt(2)−C(13)	83.7(2)			C(19)−Pt(2)−P(4)	90.51(18)
C(13)−Pt(2)−P(4)	173.36(18)			C(19)−Pt(2)−P(2)	174.62(18)
C(13)−Pt(2)−P(2)	91.33(17)			P(4)−Pt(2)−P(2)	94.58(6)
P(1)−Pd−P(2)	106.64(7)			P(1)−Pd−P(3)	161.97(7)
P(2)−Pd−P(3)	91.32(6)			P(1)−Pd−Pt(1)	52.22(5)
P(2)−Pd−Pt(1)	158.55(5)			P(3)−Pd−Pt(1)	109.76(5)
Pd−P(1)−Pt(1)	78.16(6)			Pd−P(2)−Pt(2)	117.35(7)
P(4)−P(3)−Pd	104.65(8)			P(3)−P(4)−Pt(2)	104.87(8)

Table 4. Selected Bond Distances (Angstroms) and Angles (Degrees) for $[PdPt_2Tl(\mu\text{-}Br)(\mu\text{-}PPh_2)_2(\mu\text{-}Ph_2P\text{-}PPh_2)(R_F)_4]\cdot 2.25CH_2Cl_2$ (**7**·$2.25CH_2Cl_2$)

Pt(1)−C(1)	2.055(7)	Pt(1)−C(7)	2.064(7)	Pt(1)−P(2)	2.2668(18)
Pt(1)−P(1)	2.3585(19)	Pt(2)−C(19)	1.997(7)	Pt(2)−C(13)	2.081(7)
Pt(2)−P(4)	2.3199(18)	Pt(2)−Br	2.5384(8)	Pt(2)−Tl	2.9392(5)
Pd−P(1)	2.3010(18)	Pd−P(3)	2.3184(19)	Pd−P(4)	2.3430(19)
Pd−Br	2.5676(9)	P(2)−P(3)	2.228(3)		
C(1)−Pt(1)−C(7)	87.5(3)			C(1)−Pt(1)−P(2)	88.89(18)
C(7)−Pt(1)−P(2)	175.1(2)			C(1)−Pt(1)−P(1)	177.58(19)
C(7)−Pt(1)−P(1)	91.22(19)			P(2)−Pt(1)−P(1)	92.53(6)
C(19)−Pt(2)−C(13)	88.2(3)			C(19)−Pt(2)−P(4)	98.1(2)
C(13)−Pt(2)−P(4)	172.9(2)			C(19)−Pt(2)−Br	179.1(2)
C(13)−Pt(2)−Br	91.2(2)			P(4)−Pt(2)−Br	82.36(5)
C(19)−Pt(2)−Tl	103.5(2)			C(13)−Pt(2)−Tl	91.4(2)
P(4)−Pt(2)−Tl	90.06(5)			Br−Pt(2)−Tl	77.24(2)
P(1)−Pd−P(3)	91.88(7)			P(1)−Pd−P(4)	98.33(7)
P(3)−Pd−P(4)	169.27(7)			P(1)−Pd−Br	179.48(6)
P(3)−Pd−Br	88.48(5)			P(4)−Pd−Br	81.29(5)
Pt(2)−Br−Pd	81.89(2)			Pd−P(1)−Pt(1)	119.52(7)
P(3)−P(2)−Pt(1)	106.39(9)			P(2)−P(3)−Pd	114.12(9)

Table 5. Selected Bond Distances (Angstroms) and Angles (Degrees) for $[AgPdPt_2(\mu\text{-}Br)(\mu\text{-}PPh_2)_2(\mu\text{-}Ph_2P\text{-}PPh_2)(R_F)_4(PPh_3)]\cdot 1.5n\text{-}C_6H_{14}$ (**8**·$1.5n\text{-}C_6H_{14}$)

Pt(1)−C(7)	2.066(7)	Pt(1)−C(1)	2.074(7)	Pt(1)−P(2)	2.276(2)
Pt(1)−P(1)	2.3687(18)	Pt(2)−C(19)	1.994(6)	Pt(2)−C(13)	2.047(6)
Pt(2)−P(4)	2.3025(19)	Pt(2)−Br	2.5512(8)	Pt(2)-Ag	2.7519(8)
Pt(2)−Pd	3.2458(6)	Pd−P(1)	2.3037(19)	Pd−P(3)	2.320(2)
Pd−P(4)	2.3321(19)	Pd−Br	2.6040(9)	Ag−P(5)	2.372(2)
Ag−Br	2.7899(11)	P(2)−P(3)	2.234(3)		
C(7)−Pt(1)−C(1)	82.9(3)			C(7)−Pt(1)−P(2)	177.70(19)
C(1)−Pt(1)−P(2)	94.8(2)			C(7)−Pt(1)−P(1)	91.89(19)
C(1)−Pt(1)−P(1)	173.7(2)			P(2)−Pt(1)−P(1)	90.40(7)
C(19)−Pt(2)−C(13)	89.5(3)			C(19)−Pt(2)−P(4)	95.3(2)
C(13)−Pt(2)−P(4)	174.2(2)			C(19)−Pt(2)−Br	178.1(2)
C(13)−Pt(2)−Br	92.3(2)			P(4)−Pt(2)−Br	82.85(5)
C(19)−Pt(2)−Ag	116.0(2)			C(13)−Pt(2)−Ag	96.5(2)
P(4)−Pt(2)−Ag	84.31(5)			Br−Pt(2)−Ag	63.35(2)
C(19)−Pt(2)−Pd	127.1(2)			C(13)−Pt(2)−Pd	128.3(2)
P(4)−Pt(2)−Pd	45.92(5)			Br−Pt(2)−Pd	51.708(19)
Ag−Pt(2)−Pd	96.93(2)			P(1)−Pd−P(3)	90.81(7)
P(1)−Pd−P(4)	99.32(7)			P(3)−Pd−P(4)	168.53(7)
P(1)−Pd−Br	178.03(5)			P(3)−Pd−Br	88.56(5)
P(4)−Pd−Br	81.13(5)			P(1)−Pd−Pt(2)	131.25(5)
P(3)−Pd−Pt(2)	129.49(5)			P(4)−Pd−Pt(2)	45.17(5)
Br−Pd−Pt(2)	50.26(2)			P(5)−Ag−Pt(2)	159.00(6)
P(5)−Ag−Br	137.31(6)			Pt(2)−Ag−Br	54.81(2)
Pt(2)−Br−Pd	78.04(2)			Pt(2)−Br−Ag	61.84(2)
Pd−P(1)−Pt(1)	118.86(8)			P(3)−P(2)−Pt(1)	104.79(9)
P(2)−P(3)−Pd	113.93(9)				
Pt(2)−P(4)−Pd	88.91(7)				

Pt(2)−Pd distance of 3.346(1) Å and a bridging bromine ligand. In fact, the whole Pt−Pd–Pt skeleton is very similar to those found in the precursor **5**, the dihedral angles being 29.8(1)° for the best platinum(1) and palladium planes and

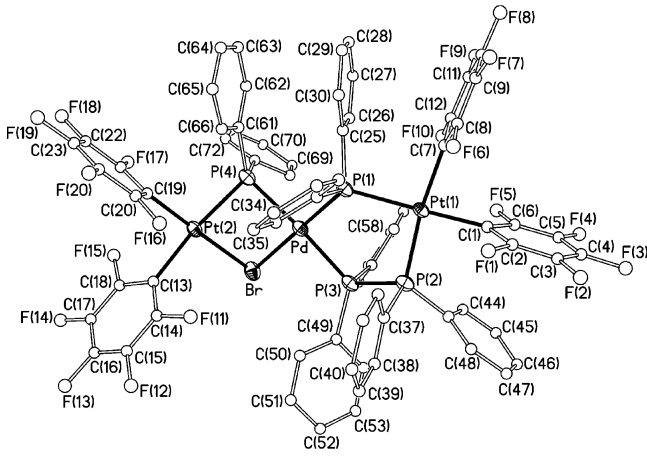

Figure 1. Molecular structure of the anion of complex $[NBu_4][(R_F)_2Pt(\mu\text{-}PPh_2)(\mu\text{-}Br)Pd(\mu\text{-}PPh_2)(\mu\text{-}P_2Ph_4)Pt(R_F)_2]$ (**5**).

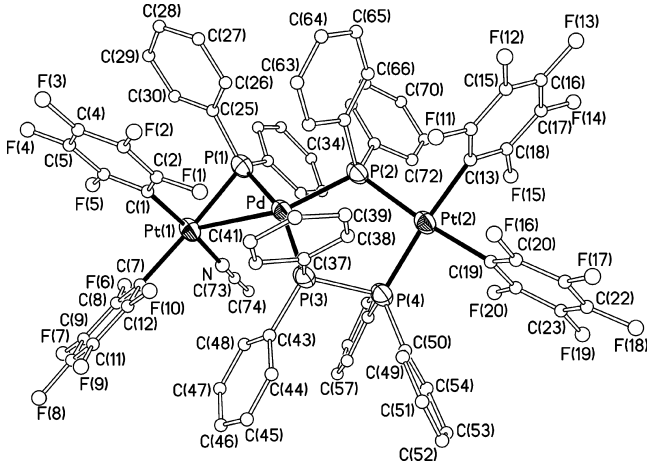

Figure 2. Molecular structure of the complex $[(R_F)_2(CH_3CN)Pt(\mu\text{-}PPh_2)Pd(\mu\text{-}PPh_2)(\mu\text{-}P_2Ph_4)Pt(R_F)_2]$ (**6**).

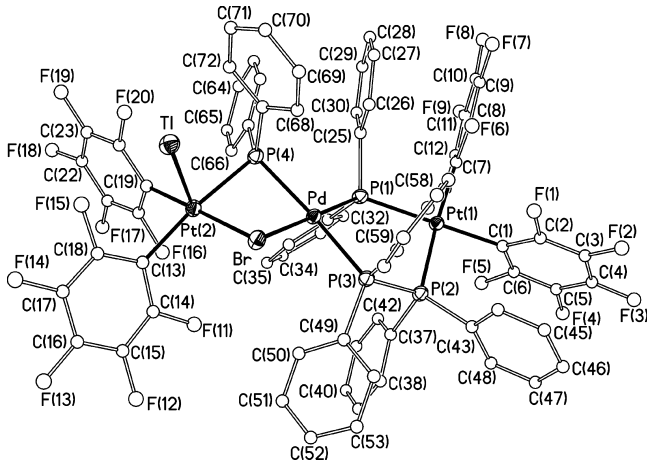

Figure 3. Molecular structure of the complex $[PdPt_2Tl(\mu\text{-}Br)(\mu\text{-}PPh_2)_2(\mu\text{-}Ph_2P\text{-}PPh_2)(R_F)_4]$ (**7**).

48.0(1)° for the platinum(2) and palladium ones. The most relevant feature of **7** is the presence of a thallium atom bonded to platinum(2). The Pt(2)−Tl distance is 2.939(1) Å, and the angle between the Pt(2)−Tl line and the perpendicular to the best Pt(2) coordination plane is 12.9(1)°. All of these geometric parameters are in agreement with a Pt−Tl bond.[17–34] A noteworthy feature of this structure is the presence of *o*-F···Tl contacts, with distances Tl−F(15)

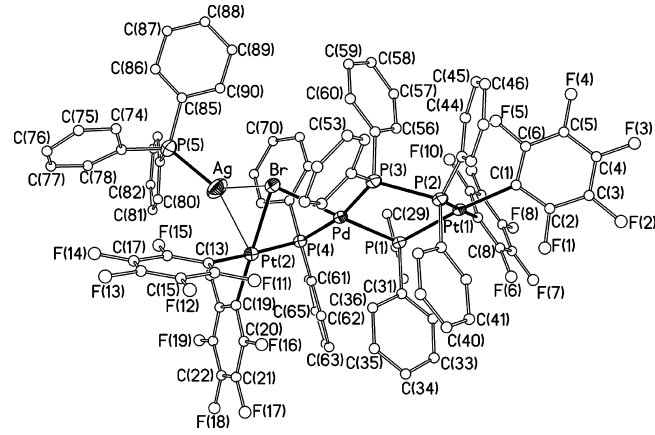

Figure 4. Molecular structure of the complex $[AgPdPt_2(\mu\text{-}Br)(\mu\text{-}PPh_2)_2(\mu\text{-}Ph_2P\text{-}PPh_2)(R_F)_4(PPh_3)]$ (**8**).

= 2.951(7) Å and Tl−F(20) = 3.014(7) Å, which are in the range found in platinum(II) complexes containing Pt−Tl bonds,[19,22,23,27] or thallium complexes containing intra-[37–40] or intermolecular F···Tl contacts.[26,29,37,41–45] These *o*-F···Tl contacts are also detected in solution in the ^{19}F NMR spectra of **5** (below).

The structure of $[AgPdPt_2(\mu\text{-}Br)(\mu\text{-}PPh_2)_2(\mu\text{-}Ph_2P\text{-}PPh_2)(R_F)_4(PPh_3)]$ (**8**) (Figure 4) shows a Pt−Pd–Pt core very similar to **5** and **7**. The dihedral angles are 36.6(1)° for the best platinum(1) and palladium planes and 54.1(1)° for the platinum(2) and palladium ones. **8** contains a Pt → Ag bond with an intermetallic distance of 2.752(1) Å. The Pt−Ag line forms an angle of 26.8(1)° with the perpendicular to the best platinum coordination plane. The formation of complexes with Pt−Ag bonds perpendicular to the platinum plane is well established,[46–51] but halo derivatives with Pt−Ag bond are scarcer[46] because precipitation of the silver halide is usually observed, as in the formation of **6**. A remarkable feature of the structure of **8** is the observation that the silver

(37) Han, R.; Ghosh, P.; Desrosiers, P. J.; Trofimenko, S.; Parkin, G. J. *Dalton Trans.* **1997**, 3713–3718.
(38) Becker, C.; Kieltsch, I.; Broggini, D.; Mezzetti, A. *Inorg. Chem.* **2003**, *42*, 8417–8429.
(39) Fernández, E. J.; Laguna, A.; López-de-Luzuriaga, J. M.; Montiel, M.; Olmos, M. E.; Pérez, J. *Organometallics* **2005**, *24*, 1631–1637.
(40) Sarazin, Y.; Hughes, D.; Kaltsoyannis, N.; Wright, J. A.; Bochman, M. *J. Am. Chem. Soc.* **2007**, *129*, 881–894.
(41) Bakar, W. A. W. A.; Davidson, J. L.; Lindsell, W. E.; McCullough, K. J.; Muir, K. W. *J. Chem. Soc., Dalton Trans.* **1989**, 991–1002.
(42) Hill, N. J.; Levason, W.; Light, M. E.; Reid, G. *Chem. Commun.* **2003**, 110–111.
(43) Connelly, N. G.; Hicks, O. M.; Lewis, G. R.; Moreno, M. T.; Orpen, A. G. *Dalton Trans.* **1998**, 1913–1918.
(44) Childress, M. V.; Millar, D.; Alam, T. M.; Kreisel, K. A.; Yap, G. P. A.; Zakharov, L. N.; Golen, J. A.; Rheingold, A. L.; Doerrer, L. H. *Inorg. Chem.* **2006**, *45*, 3864–3877.
(45) Reger, D. L.; Collins, J. E.; Layland, R.; Adams, R. D. *Inorg. Chem.* **1996**, *35*, 1372–1376.
(46) Forniés, J.; Martín, A. In *Metal Clusters in Chemistry*; Braunstein, P., Oro, L. A., Raithby, P. R., Eds.; Wiley-VCH: Weinheim, 1999; Vol. *1*.
(47) Alonso, E.; Forniés, J.; Fortuño, C.; Martín, A.; Orpen, A. G. *Organometallics* **2003**, *22*, 5011–5019.
(48) Janzen, D. E.; Mehne, L. F.; VanDerveer, D. G.; Grant, G. J. *Inorg. Chem.* **2005**, *44*, 8182–8184.
(49) Oberbeckmann-Winter, N.; Morise, X.; Braunstein, P.; Welter, R. *Inorg. Chem.* **2005**, *44*, 1391–1403.
(50) Liu, F.; Chen, W.; Wang, D. *Dalton Trans.* **2006**, 3015–3024.
(51) Falvello, L. R.; Forniés, J.; Fortuño, C.; Durán, F.; Martín, A. *Organometallics* **2002**, *21*, 2226–2234.

atoms are bonded to the bridging bromide, the Ag−Br distance being 2.790(1) Å. In fact, the location of the silver atom is such that, as indicated above, the Pt−Ag line is not perfectly orthogonal to the platinum plane, but rather the silver leans toward the bromine atom, thus causing a greater proximity between the two atoms. A similar arrangement has been found in the pentahalophenyl complexes [*trans*-$(C_6X_5)_2X'(\mu\text{-}X')PtAg(PPh_3)]^-$ (X = F, X′ = Cl;[52] X = X′ = Cl[53]) and [*trans*-$(PPh_3)(C_6X_5)X'(\mu\text{-}X')PtAg(PPh_3)]^-$ (*X* = X′ = Cl;[54] × = Cl, X′ = Br[55]). This later also has bromo as the bridging ligand, and the Ag−Br distance is shorter (2.607(1) Å), perhaps due to the presence of the bulkier PPh_2 bonded to platinum in **8**. This geometric arrangement can be regarded as a snapshot of the beginning of the halide abstraction process.

Spectroscopic Properties. All of these complexes have four inequivalent C_6F_5 groups. Their ^{19}F NMR spectra show many overlapped and broad signals, and they are not informative of the structure of the complexes. The spectrum of **5** shows four signals of equal intensity in the *o*-F region, indicating the equivalence, in solution, of the two halves of the C_6F_5 ring within each group. In **6**, the presence of the four inequivalent C_6F_5 groups is demonstrated because of the presence of four signals at high field, unambiguously assigned to the *p*-F atoms. The ^{19}F NMR spectrum of **7** in CD_2Cl_2 solution at 183 K shows seven signals in 1:2:1:1:1:1:1 intensity ratio in the region due to the *o*-F atoms in agreement with the presence of eight inequivalent atoms, two of them being isochronous. The ones that appear at higher field (−121.5 and −123.7 ppm) are broad doublets, $J^{203,205}Tl,o\text{-}F$ = 2696 and 2529 Hz, respectively. The existence of these Tl−F couplings indicate that the Tl···F interactions observed in the solid state are also present in solution at this temperature [Tl···F distances, F(15) 2.951(4) Å; F(20) 3.014(4) Å]. At room temperature, a broad signal with platinum satellites and two very broad and overlapped singlets are observed for the *o*-F atom, indicating a dynamic behavior with the loss of thallium−fluorine coupling. Similar spectroscopic features have been observed in other complexes displaying Tl···F interactions.[19,22,23,27] Analogously, the ^{19}F NMR spectrum of **8** at room temperature shows very broad, overlapped signals with platinum satellites for the *o*-F atoms, which split into six signals (1:1:3:1:1:1 intensity ratio) at 183 K. The more-intense signal is broad, and some of the platinum satellites appear overlapped. In the higher field region (*m*- and *p*-F atoms) the signals due to 12 inequivalent fluorine atoms appear overlapped. In the spectrum of the mixture of **9** and **10**, only the signals due to fluorine atoms of the $PPh_2C_6F_5$ group of **10** can be assigned (−124.5 2 *o*-F, −151.5 1 *p*-F, and −162.6 2 *m*-F atoms) because they are not masked by the fluorine signals of the $M-C_6F_5$ groups.[5–7,10]

Table 6. $^{31}P\{^1H\}$ NMR data for **5**-**10**. *J* in Hz

complex	**5**[a]	**6**[b]	**7**[a]	**8**[a,d]	**9**[e]	**10**[e,f]
δP^1	17.0	33.9	28.9	30.3	14.0	−122.5
δP^2	53.0	44.6	55.5	55.0	58.3	−149.8
δP^3	71.4	55.7	79.5	77.8	73.9	−34.0
δP^4	26.1	145.2	1.8	22.5	22.5	10.3
JP^2,P^3	191	175	198	203	187	322
JP^3,P^4	296	268	304	294	303	307
JPt^1,P^1	1881	1975	1883	1990	1867	1798
JPt^1,P^2	2400	2365	2395	2403	2441	1647
JPt^1,P^3	296	[c]	295	295	317	
JPt^2,P^4	1862	1568	1664	1531	1773	2263

[a] In $CDCl_3$ at 295 K. [b] In $CDCl_3$ at 213 K, $^2JP^1,P^4$ = 45. [c] See text. [d] δP^5 = 11.6, $^1J^{109}Ag,P^3$ = 773, $^1J^{107}Ag,P^3$ = 671. [e] In deuteroacetone at 295 K. [f] JPt^2,P^3 = 1746, JP^1,P^2 = 194, JP^1,P^3 = 36.

The $^{31}P\{^1H\}$ NMR spectra in solution of **5**−**8** and the mixture of **9** and **10** are in agreement with the structures observed (**5**−**8**) or proposed (**9** and **10**) in the solid state. All of the data extracted from these spectra are given in Table 6. The spectrum of **5** shows four signals, of which the signals due to the phosphorus atoms of the phosphido ligands, P^1 and P^4 (Scheme 2 for atom numbering) appear at 17.0 and 26.1 ppm, respectively, whereas the signals corresponding to these atoms appear in the starting material **4** at 123.6 ppm.[12] The chemical shift of P^1 and P^4 atoms are in fully agreement with the presence in solution of a bridged system $M(\mu\text{-}PPh_2)(\mu\text{-}X)M'$ without a metal−metal bond.[11,56–59] The diphosphine ligand is forming a five member ring, and the signals due to P^2 and P^3 atoms appear at a higher field (53.0 and 71.4 ppm respectively) than in the starting material **4** (80.0 ppm).[12] It is noteworthy that the coupling between the inequivalent phosphorus atoms of the diphosphine ligand, 191 Hz, is smaller than the coupling between P^3 and P^4 atoms through two bonds, 296 Hz. All of the signals show platinum satellites from which the $^1JPt,P$ or $^2JPt,P$ values can be extracted. Very similar values are obtained for the analogous **9**. The spectrum of **6** at 213 K shows the same pattern as that at room temperature but in the latter case the signals due to P^4 and P^3 atoms (Scheme 2 for atom numbering) are broad. The most relevant features of **6** compared to **5** are: (i) the shift of the P^4 signal toward lower field, 145.2 ppm, as expected for a $M(\mu\text{-}PPh_2)M'$ fragment with a metal−metal bond;[10,60,61] (ii) the signal due to P^3 shows very broad platinum satellites as a consequence of coupling with both platinum,[1] as in **5**, and with Pt^2 and, consequently, the two $^2JPt,P^3$ values can not be calculated accurately; (iii) the coupling between P^1 and P^4 is observed in **6**, probably as a consequence of the larger P^1-Pd-P^4 angle (106.6(1)° in solid state). The main difference in the $^{31}P\{^1H\}$ NMR spectrum of **7** at room temperature with respect to the starting material is the decrease in ca. 25 ppm of the chemical shift

(52) Usón, R.; Forniés, J.; Menjón, B.; Cotton, F. A.; Falvello, L. R.; Tomás, M. *Inorg. Chem.* **1985**, *24*, 4651–4656.
(53) Usón, R.; Forniés, J.; Tomás, M.; Casas, J. M.; Cotton, F. A.; Falvello, L. R. *Inorg. Chem.* **1986**, *25*, 4519–4525.
(54) Usón, R.; Forniés, J.; Tomás, M.; Ara, I.; Casas, J. M. *Inorg. Chem.* **1989**, *28*, 2388–2392.
(55) Usón, R.; Forniés, J.; Tomás, M.; Ara, I. *Inorg. Chim. Acta* **1991**, *186*, 67–71.
(56) Alonso, E.; Forniés, J.; Fortuño, C.; Martín, A.; Rosair, G. M.; Welch, A. J. *Inorg. Chem.* **1997**, *36*, 4426–4431.
(57) Alonso, E.; Forniés, J.; Fortuño, C.; Tomás, M. *J. Chem. Soc., Dalton Trans.* **1995**, 3777–3784.
(58) Ara, I.; Chaouche, N.; Forniés, J.; Fortuño, C.; Kribii, A.; Tsipis, A. C.; Tsipis, C. A. *Inorg. Chim. Acta* **2005**, *358*, 1377–1385.
(59) Alonso, E.; Forniés, J.; Fortuño, C.; Martín, A.; Orpen, A. G. *Organometallics* **2003**, *22*, 2723–2728.
(60) Alonso, E.; Forniés, J.; Fortuño, C.; Martín, A.; Orpen, A. G. *Organometallics* **2000**, *19*, 2690–2697.
(61) Alonso, E.; Forniés, J.; Fortuño, C.; Martín, A.; Orpen, A. G. *Organometallics* **2001**, *20*, 850–859.

of P^4 atom along with the decrease in ca. 200 Hz in the $^1JPt^2,P^4$. Analogous decreases in the ^1JPt,P values have been observed in phosphino derivatives after complexation with Tl^+.[23,29,34,62] No coupling between ^{31}P and thallium was observed in the phosphido derivative **7**, which is consistent with the finding of other authors.[18,23,29,33,34,62] In the spectrum of **8**, the signal due to the P^5 atom appears as two doublets (^{107}Ag and ^{109}Ag isotopes, $I = {}^1/_2$) somewhat broadened at the base due to the poorly resolved coupling of P^5 with the Pt^2 atom.

The ^1H NMR spectra of **5** and of the mixture of **9** and **10** show signals due to the hydrogen atoms of the phenyl groups along with those due to the counterion $[NBu_4]^+$. Their relative intensities are in agreement with the anionic nature of the complexes.

Concluding Remarks

The unsaturated trinuclear **4** (44 valence electron count) easily adds a bromo ligand, yielding the saturated (48 electrons) **5**. The process is reversible, and the addition of M(I) salts (M = Tl, Ag) produces (after the elimination of MBr) the cluster **4** through its acetonitrile adduct **6**, that is, the cleavage of the P−P bond and the formation of the P−C one rendering PPh_2R_F is not observed through the addition/elimination of halide.

The addition of I_2 to the heterotrinuclear platinum/palladium(II) complex $[(R_F)_2Pt^{II}(\mu\text{-}PPh_2)_2Pd^{II}(\mu\text{-}PPh_2)_2Pt^{II}(R_F)_2]^{2-}$ indicates that, from the proposed M(III) intermediate **1b** in presence of I^- both reductive coupling processes, the formation of the P−P bond and of the P−C bond, could take place. In the latter process, the cleavage of the Pd−P and Pt−C bonds has to be accompanied with the formation of the Pd−I and Pt−I bonds.

Finally, in a more general context, the 1:1 adducts **7** and **8** provide structural evidence for metal−metal bonded intermediates in the processes of halide abstraction.

Experimental Section

General Comments. Carbon, hydrogen, and nitrogen analyses were performed with a PerkinElmer 240B microanalizer. IR spectra were recorded on a PerkinElmer Spectrum One spectrophotometer (Nujol mulls between polyethylene plates in the range 4000−350 cm^{-1}). NMR spectra were recorded on a Varian Unity 300 or a Bruker Avance 400 spectrometers with $SiMe_4$, $CFCl_3$, and 85% H_3PO_4 as external references for ^1H, ^{19}F, and ^{31}P, respectively. Literature methods were used to prepare the starting material $[PdPt_2(\mu\text{-}PPh_2)_2(\mu\text{-}Ph_2P\text{-}PPh_2)(R_F)_4]$,[12] $[NBu_4]_2[(R_F)_2Pt(\mu\text{-}PPh_2)_2Pd(\mu\text{-}PPh_2)_2Pt(R_F)_2]$,[4] and $[AgOClO_3(PPh_3)]$.[63]

Caution! *Perchlorate salts of metal complexes with organic ligands are potentially explosive. Only small amounts of materials should be prepared, and these should be handled with great caution.*

Synthesis of $[NBu_4][(R_F)_2Pt(\mu\text{-}PPh_2)(\mu\text{-}Br)Pd(\mu\text{-}PPh_2)(\mu\text{-}P_2Ph_4)Pt(R_F)_2]$ 5. To a red suspension of **4** (0.300 g, 0.157 mmol) in acetone (20 mL) NBu_4Br (0.051 g, 0.158 mmol) was added. The orange-red solution was stirred for 5 h and evaporated to ca. 2 mL. ^{i}PrOH (3 mL) was added and an orange-yellow solid, **5**, crystallized, which was filtered off and washed with ^{i}PrOH (3 × 0.5 mL), 0.243 g, 69% yield. Anal. Found (Calcd for $BrC_{88}F_{20}H_{76}NP_4PdPt_2$): C, 47.8 (47.7); H, 3.3 (3.4); N, 0.6 (0.6). $\Lambda_M = 48$ ohm^{-1}cm^{2}mol^{-1}. IR (cm^{-1}): 802, 787 and 776 (X-sensitive C_6F_5).[64,65] ^{19}F NMR room temperature ($CDCl_3$, 282.4 MHz): δ −115.7 [2 *o*-F, $^3J(^{195}Pt, F)$ = 291 Hz], −116.2 [2 *o*-F, $^3J(^{195}Pt, F)$ cannot be measured], −116.7 [2 *o*-F, $^3J(^{195}Pt, F)$ cannot be measured], −117.6 [2 *o*-F, $^3J(^{195}Pt, F)$ = 541 Hz],−163.9 (1 *p*-F), from −164.6 to −164.9 (6 F), −165.3 (1 *p*-F), −165.6 (2 F), −167.4 (2 F).

Synthesis of $[(R_F)_2(CH_3CN)Pt(\mu\text{-}PPh_2)Pd(\mu\text{-}PPh_2)(\mu\text{-}P_2Ph_4)Pt(R_F)_2]$ 6. To an orange solution of **5** (0.150 g, 0.067 mmol) in acetonitrile (15 mL) $AgClO_4$ (0.027 g, 0.065 mmol) was added. Instantaneously, the color of the solution became somewhat lighter and a yellow solid began to crystallize. After two hours stirring in the dark, a yellow solid was filtered off. CH_2Cl_2 (20 mL) was added to the solid and the bright pink solution was filtered through Celite. The solution was evaporated to ca. 1 mL, ^{i}PrOH (3 mL) was added, and **6** crystallized as an orange-pink solid, which was filtered off, washed with ^{i}PrOH (2 × 0.5 mL), and dried under vacuum, 0.046 g, 37% yield. Anal. Found (calcd for $C_{74}F_{20}H_{43}NP_4PdPt_2$): C, 45.34 (45.6); H, 1.8 (2.2); N, 0.6 (0.7). IR (cm^{-1}): 2322 (νC≡ N);[66] 806, 793, and 781 (X-sensitive C_6F_5). ^{19}F NMR room temperature ($CDCl_3$, 282.4 MHz): δ −116.5 (4 *o*-F), −117.1 (2 *o*-F), −118.5 (2 *o*-F), −159.7 (1 *p*-F), −161.0 (1 *p*-F), −162.6 (1 *p*-F), −163.1 (1 *p*-F) −163.4 (4 *m*-F), −164.0 (2 *m*-F), −164.4 (2 *m*-F).

Synthesis of $[PdPt_2Tl(\mu\text{-}Br)(\mu\text{-}PPh_2)_2(\mu\text{-}Ph_2P\text{-}PPh_2)(R_F)_4]$ 7. To an orange solution of **5** (0.150 g, 0.067 mmol) in CH_2Cl_2 (15 mL) $TlPF_6$ (0.024 g, 0.069 mmol) was added, and the mixture was stirred in the dark for 6 h. The orange solution was filtered through Celite, evaporated to ca. 8 mL, and passed through silica gel (2 cm^2 × 10 mL). The filtrate was evaporated to ca. 1 mL, ^{i}PrOH (8 mL) was added, and **7** crystallized as a yellow solid, which was filtered off and washed with ^{i}PrOH (2 × 0.5) mL, 0.076, 52% yield. Anal. Found (Calcd for $BrC_{72}F_{20}H_{40}P_4PdPt_2Tl$): C, 39.4 (39.5); H, 1.8 (1.8). IR (cm^{-1}): 805, 791, and 780 (X-sensitive C_6F_5). ^{19}F NMR 183 K ($CDCl_3$, 376.5 MHz): δ −112.4 [1 *o*-F, $^3J(^{195}Pt, F)$ = 292 Hz], −115.8 [2 *o*-F, $^3J(^{195}Pt, F)$ = 255 Hz], −117.1 [1 *o*-F, $^3J(^{195}Pt, F)$ = 322 Hz], −118.3 [1 *o*-F, $^3J(^{195}Pt, F)$ = 456 Hz],−119.4 [1 *o*-F, $^3J(^{195}Pt, F)$ = 361 Hz], −121.5 [1 *o*-F, $J(^{203,205}Tl, F)$ = 2696 Hz], −123.7 [1 *o*-F, $J(^{203,205}Tl, F)$ = 2529 Hz], −160.8 (1 F), −162.2 (1 F), −163.0 (2 F), −163.4 (2 F), −163.8 (1 F), −164.6 (3 F), −165.0 (1 F), −165.4 (1 F).

Synthesis of $[AgPdPt_2(\mu\text{-}Br)(\mu\text{-}PPh_2)_2(\mu\text{-}Ph_2P\text{-}PPh_2)(R_F)_4)(PPh_3)]$ 8. To an orange solution of **5** (0.150 g, 0.067 mmol) in CH_2Cl_2 (15 mL) $[AgOClO_3(PPh_3)]$ (0.032 g, 0.067 mmol) was added, and the mixture was stirred in the dark for 30 min. The orange solution was filtered through Celite and evaporated to ca. 2 mL. ^{i}PrOH (3 mL) was added and **8** crystallized as a yellow solid, which was filtered off and washed with ^{i}PrOH (2 × 1) mL, 0.118, 74% yield. Anal. Found (Calcd for $BrC_{90}F_{20}H_{55}P_4AgPdPt_2$): C, 45.5 (45.8); H, 2.3 (2.3). IR (cm^{-1}): 806, 791 and 780 (X-sensitive C_6F_5). ^{19}F NMR 183 K ($CDCl_3$, 282.4 MHz): δ −111.6 (1 *o*-F), −115.3 (1 *o*-F), −117.0 (3 *o*-F), −117.6 (1 *o*-F), −118.8 (1 *o*-F), −120.0 (1 *o*-F), −161.1 (1 F), −161.8 (1 F), from −162.9 to −165.5 (10 F).

(62) Catalano, V. C.; Bennett, B. L.; Muratidis, S.; Noll, B. C. *J. Am. Chem. Soc.* **2001**, *123*, 173–174.
(63) Cotton, F. A.; Falvello, L. R.; Usón, R.; Forniés, J.; Tomás, M.; Casas, J. M.; Ara, I. *Inorg. Chem.* **1987**, *26*, 1366–1370.
(64) Maslowsky, E. J. *Vibrational Spectra of Organometallic Compounds; Wiley: New York*, 1997.
(65) Usón, R.; Forniés, J. *Adv. Organomet. Chem.* **1988**, *28*, 219–297.
(66) Murahashi, T.; Nagai, T.; Okuno, T.; Matsutani, T.; Kurosawa, H. *Chem. Commun.* **2000**, 1689–1690.

Reaction of $[NBu_4]_2[(R_F)_2Pt(\mu\text{-}PPh_2)_2Pd(\mu\text{-}PPh_2)_2Pt(R_F)_2]$ with I_2. To an orange solution of $[NBu_4]_2[(R_F)_2Pt(\mu\text{-}PPh_2)_2Pd(\mu\text{-}PPh_2)_2Pt(R_F)_2]$ (0.200 g, 0.084 mmol) in acetonitrile (20 mL) at room temperature was added a solution of I_2 (0.021 g, 0.084 mmol) in acetonitrile. After 7 h of stirring at room temperature, the red solution was evaporated to ca. 1 mL, ^{i}PrOH (6 mL) was added, and a mixture of **9** and **10** (ca. 1:1 molar ratio) crystallized, which was stirred for 2 h, filtered off, and washed with ^{i}PrOH (2 × 0.5 mL): 0.105 g, 55% yield. Anal. Found (Calcd for $C_{88}F_{20}H_{76}INP_4PdPt_2$): C, 46.4 (46.4); H, 3.1 (3.3); N, 0.8 (0.6). In another experiment: to an orange solution of $[NBu_4]_2[(R_F)_2Pt(\mu\text{-}PPh_2)_2Pd(\mu\text{-}PPh_2)_2Pt(R_F)_2]$ (0.250 g, 0.104 mmol) in acetonitrile (20 mL) at 233 K was added a solution of I_2 (0.026 g, 0.104 mmol) in acetonitrile. After 1 h stirring at 233 K, the solution was evaporated to ca. 2 mL, and a solid crystallized that was filtered off and dried under vacuum. The orange-pink solid was dissolved in CH_2Cl_2 (20 mL), and after 10 min stirring at room temperature the solution was evaporated, keeping this temperature to ca. 2 mL and left in the freezer for 20 h. The orange solid **4** was filtered off, washed with cold CH_2Cl_2 (2 × 0.5 mL), and dried under vacuum: 0.095 g, 48% yield.

X-ray Structure Determinations. Crystal data and other details of the structure analysis are presented in Table 1. Suitable crystals of $\mathbf{5}\cdot CH_2Cl_2\cdot 0.5n\text{-}C_6H_{14}$, $\mathbf{6}\cdot 1.5CH_2Cl_2$, $\mathbf{7}\cdot 2.25CH_2Cl_2$, and $\mathbf{8}\cdot 1.5n\text{-}C_6H_{14}$ were obtained by slow diffusion of *n*-hexane into a CH_2Cl_2 solution of the complexes. Crystals were mounted at the end of a glass fiber. In all of the cases, the diffraction data were collected in a Bruker Smart Apex diffractometer. Unit cell dimensions were determined from the positions of 4725, 7751, 936, and 1018 reflections from the main data set respectively. For all of the structures, the diffraction frames were integrated using the *SAINT* package[67] and corrected for absorption with *SADABS*.[68] Lorentz and polarization corrections were applied in all cases.

The structures were solved by Patterson and Fourier methods. All refinements were carried out using the *SHELXL-97* program.[6970] All non-hydrogen atoms were assigned anisotropic displacement parameters and refined without positional constraints except as noted below. All hydrogen atoms were constrained to idealized geometries and assigned isotropic displacement parameters 1.2 times the U_{iso} value of their attached carbon atoms (1.5 times for methyl hydrogen atoms). For $\mathbf{5}\cdot CH_2Cl_2\cdot 0.5C_6H_{14}$, a molecule of *n*-hexane was found lying around an inversion center and disordered over two sets of positions refined with occupancy 0.5. No hydrogen atoms were added on the disordered *n*-hexane molecule. For $\mathbf{6}\cdot 1.5CH_2Cl_2$, two molecules of dichloromethane solvate were found and their atoms refined with a partial occupancy of 0.75. One of the molecules has the chlorine atoms disordered over two sets of positions that were refined with partial occupancy of 0.375. No hydrogen atoms were added on this disordered molecule. The C−Cl distances of both dichloromethane molecules were restrained to sensible values. For $\mathbf{7}\cdot 2.25CH_2Cl_2$, three disordered molecules of CH_2Cl_2 were found and refined with partial occupancy 1, 0.75, and 0.50. Some of the geometric parameters of these molecules were restrained to accepted values, and common sets of thermal anisotropic parameters were used in some cases. No hydrogen atoms were added on the disordered CH_2Cl_2 molecules. For $\mathbf{8}\cdot 1.5n\text{-}C_6H_{14}$, one of the pentafluorophenyl groups [C(13)] is disordered over two positions, which share the ipso C(1) atom and that were refined with 0.6/0.4 partial occupancies. Weak restraints were applied in the geometry of these groups. One of the phenyl rings of the PPh_3 ligand [C(73)] is disordered over two positions, which share the ipso C(73) and the para C(76) atoms and that were refined with 0.5 partial occupancy each. Weak restraints were applied in the geometry of these rings. Several *n*-hexane molecules were found in the structure and modeled as follows. A half-molecule (C(91), C(92), and C(93)) placed near an inversion center that generates the rest of the molecule, with the total occupancy being 0.5. A complete molecule [C(94) to C(99)] refined with 0.50 partial occupancy. Two other complete molecules refined with 0.25 partial occupancy. In all four moieties, the bond distances were constrained to acceptable values. For the later three, no anistropic displacement parameters were used for their carbon atoms. Full-matrix least-squares refinement of these models against F^2 converged to final residual indices given in Table 1.

Acknowledgment. This work was supported by the Spanish MEC (DGI)/FEDER (Project CTQ2005-08606-C02-01) and the Gobierno de Aragón (Grupo de Excelencia: Química Inorgánica y de los Compuestos Organometálicos). S.I. acknowledges the Ministerio de Educación y Ciencia for a grant.

Supporting Information Available: Further details of the structure determinations of $\mathbf{5}\cdot CH_2Cl_2\cdot 0.5n\text{-}C_6H_{14}$, $\mathbf{6}\cdot 1.5CH_2Cl_2$, $\mathbf{7}\cdot 2.25CH_2Cl_2$, and $\mathbf{8}\cdot 1.5n\text{-}C_6H_{14}$ including atomic coordinates, bond distances and angles, and thermal parameters. This material is available free of charge via the Internet at http://pubs.acs.org.

IC800294C

(67) *SAINT*, version 5.0; Bruker Analytical X-ray Systems: Madison, WI.
(68) Sheldrick, G. M.; *SADABS Empirical Absorption Program*; University of Göttingen: Göttingen, Germany, 1996.
(69) Sheldrick, G. M.; *SHELXL-97: A Program for Crystal Structure Determination*; University of Göttingen: Göttingen, Germany, 1997.
(70) Chaouche, N.; Forniés, J.; Fortuño, C.; Kribii, A.; Martín, A. *J. Organomet. Chem.* **2007**, *692*, 1168–1172.